Flyrock Range & Fragment Size Prediction

Cameron K. McKenzie, Blastechnology, Australia

Abstract

Flyrock is a complex issue involving interaction between the charging crew, the blast design, and the local geology, and once conditions on the shot meet certain criteria, the probability of a flyrock incident becomes unacceptably high. It is essential that flyrock awareness be built into the blast design process, requiring an engineering approach to understanding and controlling the outcomes and managing the associated risks.

Based on previous studies of flyrock and published literature relating to fragment motion at high velocity in air, the equations to predict maximum flyrock range, and the size of particle achieving the maximum range, for blasts of varying rock density, hole diameter, explosive density, and state of confinement have been developed. These equations, and other associated correlations, permit the flyrock footprints to be established for any charge configuration, in any size blasthole, in rock of any density, and with particles of any known shape factor. The equations developed, and the mechanisms they reflect, allow engineers to go a long way towards understanding the primary factors controlling flyrock generation, including the rock mass, the blast design, and the quality of blast design implementation, i.e. the human factor. The paper presents guidelines as regards use of the equations to establish personnel clearance distances as a function of charge design and implementation, and equations to estimate appropriate stemming lengths when blasting must be conducted close to occupied or sensitive structures. The equations are amenable to definition of, and quantification of Flyrock Risk.

Background

The task of evaluating flyrock risk ultimately boils down to a question of how far rock fragments are likely to be projected as a function of blast design. This inevitably leads to methods of estimating flyrock ejection velocities and the resulting projection distances of fragments of various sizes, and making recommendations about blast design based on estimated projection velocities of fragments. A reliable flyrock model must therefore be able to provide reasonably accurate estimations of both projection velocity and projection distance, ideally as a function of the fragment size and blast design.

Several studies of flyrock projection have been conducted and reported (Roth 1981, Workman & Calder 1994, Richards & Moore 2006), using simple kinematic equations to describe the motion of rock particles after ejection from either blasthole collars or from the free face. St George & Gibson (2001) appear to be the most notable recent exception, presenting more realistic equations to describe flyrock motion and to predict flyrock range. Avoiding the task of defining the differences between flyrock and normal rock displacements during the different types of blasting operations, flyrock is generally considered problematic when projection distances exceed, or even come close to clearance distances, typically several hundred metres. Using kinematic equations, it is clear that launch velocities must be in excess of 50 metres per second in order to achieve projection distances in excess of 250 metres, and to achieve distances in excess of 500 metres, as are commonly reported in literature, velocities must be in excess of 75 metres per second. To assess the validity of simple kinematic models as a way to model flyrock motion, velocities in the range 50 to 100 m/s therefore need to be analysed and the estimated paths and projection distances of fragments compared with more realistic particle motion, under the influence of air resistance.

Using the equations of motion proposed by Chernigovskii (1985) to calculate flight paths under the influence of air resistance, the difference between realistic models of particle motion in air, and simple kinematic models is highlighted in Figure 1, for the case of two different size particles each with a launch velocity of 70 m/s, considered low in the realm of flyrock projection velocities. Note that the kinematic models predict the same maximum projection distance for all particle sizes, whereas with the more realistic models, maximum projection distance is a strong function of particle size.

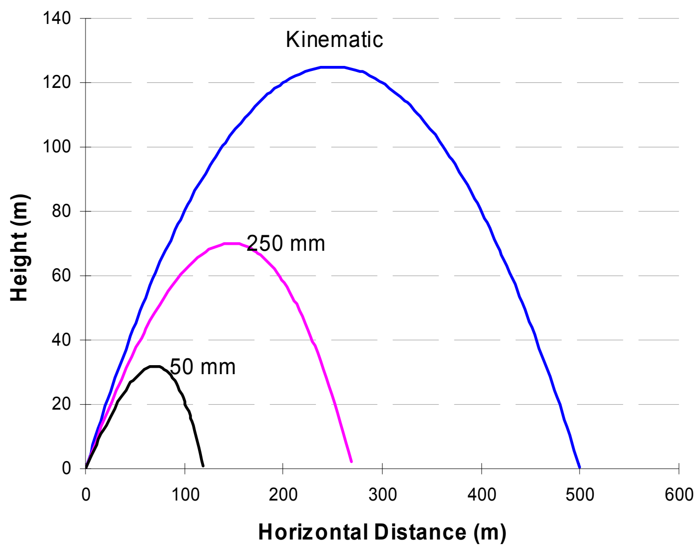

Figure 1. Difference between realistic (with air resistance) and kinematic models for estimation of maximum projection distance for fragments of 50 mm and 250 mm size (rock density = 2.6 g/cc, shape factor = 1.25, initial velocity = 70 m/s).

Clearly when typical flyrock velocities are used in both kinematic and realistic equations of motion which account for frictional resistance of air, there is a huge discrepancy between predicted projection distances, and they become exponentially greater as the launch velocity increases. Realistic models suggest that for rock fragments to travel in excess of 500 metres, launch velocities must be in excess of 200 m/s, far greater than those estimated using simple kinematic equations. If a flyrock model is unable to reliably estimate launch velocities and projection distances, then it is also unlikely to correctly identify the conditions leading to the occurrence of flyrock, or effective measures to control it. The very major discrepancies between kinematic predictions of projection distance and projection velocity and realistic predictions demand that credible flyrock models do not use simple kinematic equations of motion – a conclusion supported in the recent work by St George and Gibson (2001). Furthermore, the kinematic equations suffer the disadvantage of not providing any information about the size of fragments being projected.

The steps presented in this paper to model flyrock from blasting can be summarised as:

1. Estimate the launch velocity of fragments based on the depth of burial of the charge, rock density, and fragment size, using an impulse equation;
2. Estimate the maximum range of rock fragments as a function of the launch velocity and the fragment shape factor using equations of motion which incorporate the effects of air resistance;
3. Estimate the size of fragment capable of achieving maximum projection (depending on launch angle), as a function of rock density and fragment shape factor;
4. Use the above information to quantify risk as a function of separation distance from the blast, and the charge configuration.

Realistic Flyrock Motion

Lundborg (1974), Lundborg *et al* (1975) undertook a series of experimental and theoretical analyses of flyrock behaviour, using impulse equations to estimate particle launch velocities, and realistic equations of motion incorporating the effect of air resistance, as evidenced by the particle size dependence of the maximum projection distances in their graphs. Lundborg's study, however, was conducted in granite, using crater blast charge configurations, and many of his results are specific to that rock type only, and to that charge configuration only. The model derived for predicting maximum range from crater blasts in granite was:

$$Range = 260\,\phi^{0.667} \qquad (1)$$

and the impulse equation developed to describe the initial velocity of projected granite fragments was:

$$V_0 = 10\left(\frac{\phi}{x_f}\right)\left(\frac{2.6}{\rho_r}\right) \qquad (2)$$

It must be noted that these equations involved mixed units, with hole diameter, ø, expressed in inches, particle size x_f in metres, velocity of projection V_0 in metres per second, and rock density ρ_r in g/cc. The coefficient of 10 is referred to in this paper as the *Velocity Coefficient*, and was determined experimentally by Lundborg for his particular rock type and charge configuration.

Lundborg *et al* (1975) further stated that maximum projection distance decreased by a factor of six in normal bench blasting (this can be shown to be equivalent to a reduction in the *Velocity Coefficient* from 10 to 0.65), and that flyrock was effectively eliminated when stemming length was equal to 40 times the hole diameter. Flyrock models should therefore be able to reproduce these observations, as a minimum requirement.

The difference between crater blasting and normal bench blasting is simply the depth of burial and dimension of the charge. Implicit in Lundborg's observations is therefore a relationship not only between the velocity of projection of rock fragments and the diameter of the charge, but also between the velocity of projection and the depth of burial of the charge. This study proposes a method to quantify that correlation, as well as extending the flyrock equations to calculate maximum projection distances for fragments of any size, density, and shape. The equations are developed to apply to rock fragments projected from the collar regions of blastholes, but with quite minor adjustments they can be applied also to the free face of bench blasting applications. It is a simple matter to extend the equations to consider projection between different benches in an open pit mining application.

Scaled Depth of Burial

The concept of the scaled depth of burial of a charge was defined during cratering experiments, and described by Chiappetta (1983), Figure 2, in which it is clear that as the scaled depth of burial of a charge is reduced (from right to left in the above images), the probability of flyrock increases, the range of projected material increases, and the velocity of projection of ejected rock fragments increases. The scaled depth of burial is defined as the length of stemming plus half the length of charge contributing to the cratering effect, divided by the cube root of the weight of explosive contained within the portion of charge contributing to the crater effect. It is calculated in either US units (SDB_{US}) or metric units (SDB_m) by the equations:

$$SDB_{US} = \frac{St + 0.042\, m\,\phi}{0.305\left(m\phi^3 \rho_{exp}\right)^{0.333}} \qquad or \qquad SDB_m = \frac{St + 0.0005\, m\,\phi}{0.00923\left(m\phi^3 \rho_{exp}\right)^{0.333}} \tag{3}$$

where *St* represents the stemming length (ft/metres), ø is the hole diameter (inches/mm), ρ_{exp} is the density of the explosive in g/cc, and *m* is the charge length expressed as a multiple of hole diameter, with a maximum value of 8 for hole diameter less than 4 inches (100 mm), and a maximum value of 10 for hole diameter greater than or equal to 4 inches.

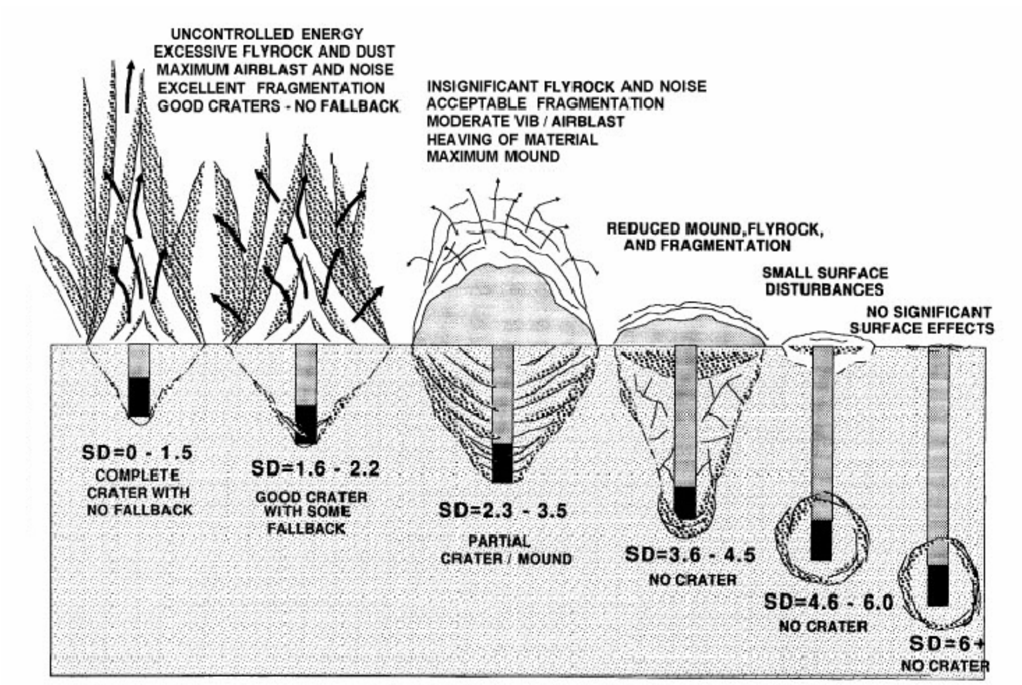

Figure 2. Scaled depth of burial (US units) as presented by Chiappetta et al (1983).

The term *m* therefore defines the length of buried charge contributing to the projection of material from the collar region as being no more than 10 times the hole diameter, implying that long charges have no greater propensity to eject flyrock than short charges.

Relating Chiappetta's graphic to the observations by Lundborg *et al* (1975), a simple empirical correlation is proposed between scaled depth of burial (*SDB*) and the *Velocity Coefficient* (K_v) noted by Lundborg:

$$SDB_{US} = 1.5, \quad K_v = 10 \ \ (crater\ blasting)$$
$$SDB_{US} = 3.5, \quad K_v = 0.65 \ \ (bench\ blasting) \qquad (4)$$
$$SDB_{US} = 6.0, \quad K_v = 0.11 \ \ (stem\ length = 40\ times\ diameter)$$

The relationships are presented graphically in Figure 3. The left hand graph shows the relationships using Lundborg's mixed-units velocity coefficient and Chiappetta's US-based SDB values, whereas the right hand graph presents the correlation in metric units for all parameters. For the sake of consistency and modernity, the remainder of this paper will use only metric equations. The assumed metric correlation is given by:

$$Velocity\ Coeff = K_v = 0.0728 \times SDB^{-3.251} \qquad (5)$$

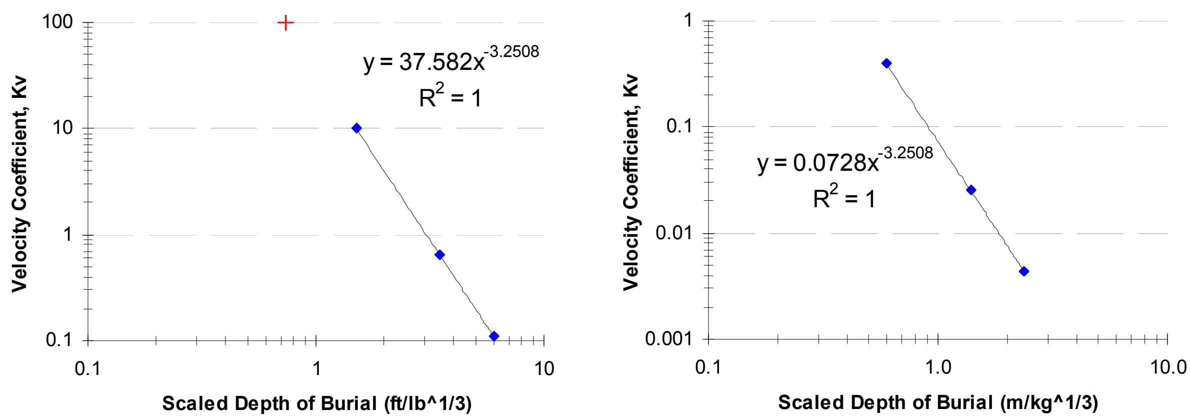

Figure 3. Assumed relation between Velocity Coefficient, K_v, and Scaled Depth of Burial, SDB.

The assumed correlation between the velocity coefficient and the scaled depth of burial therefore permits estimation of the velocity coefficient, K_v, for any charge configuration, including the effects of charge length, charge density, and the presence of air decks. It provides projection conditions totally consistent with the observations of Lundborg, covering the range of almost zero ejection to extreme ejection produced under cratering conditions, and including what Lundborg described as "normal bench blasting" configurations. The incorporation of the scaled depth of burial term therefore can be considered to completely explain the experimental results of flyrock distance and velocity (using a high speed camera) made by Lundborg *et al* (1975). Lundborg's impulse equation (2) to predict initial launch velocity of particles of different size, with particle size x_f expressed in millimetres, can therefore be rewritten:

$$V_0 = K_v \left(\frac{\phi}{x_f}\right)\left(\frac{2.6}{\rho_r}\right) = 72.8 \times SDB^{-3.251} \times \left(\frac{\phi}{x_f}\right)\left(\frac{2.6}{\rho_r}\right) \qquad (6)$$

Particle Motion Equations with Air Resistance

While it is clear that Lundborg *et al* (1975) used a model of fragment motion which included air resistance, the authors did not publish the details of that model, so that alternative sources are required. Chernigovskii (1985) reported the following equations to specifically describe the motion of blast induced flyrock fragments, using non-orthogonal reference axes.

$$z = \frac{1}{b_d} ln\left(1 + b_d V_0 t\right)$$

$$y = \frac{1}{b_d} \ln \frac{e^{2t\sqrt{b_d g}} + 1}{2e^{t\sqrt{b_d g}}}$$

$$b_d = \frac{1.3}{x_f \rho_r}$$

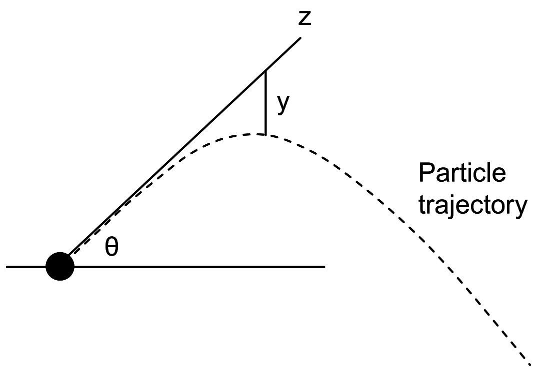

In the above equations, z is the distance (m) measured in the direction of projection of the particle, y is the distance of fall of the particle measured vertically (m), V_0 is the initial projection velocity of the particle (m/s), t is time after launch (seconds), ρ_r is the rock density (kg/m^3), x_f is the particle size (m), and g is the acceleration due to gravity (9.8 m/s^2). The constant 1.3 appearing in the third equation appears to be a shape factor. Chernigovskii describes rock fragments from blasting as having dimensions of 0.6:1:1.6. Defining the shape factor as the ratio of the surface area of the particle to that of a sphere of equal volume or weight, particles of the above dimensions are confirmed to have a shape factor of approximately 1.3, and a mass of ($x_f^3\ \rho/2.2$) kg. Hence, the constant of 1.3 in Chernigovskii's equation can be replaced by the more general shape factor term F_s to account for fragments of variable shape: $b_d = \frac{F_s}{x_f \rho_r}$, with lower values of the shape factor (i.e. shape approaching spherical) producing greater projection distances. As a note, a shape factor in the range 1.1 to 1.3 seems to describe most flyrock fragments rather well. The use of a value of unity will produce more conservative (i.e. greater) estimates of maximum projection distance for the same launch velocity.

As a verification of Chernigovskii's equations, Figure 4 compares the flyrock "footprint" curves for different blasthole diameters calculated using the above equations, with those originally presented by Lundborg *et al* (1975). The curves show the maximum projection distances for different particle sizes, scaled according to the density of granite. The agreement between the two sets of curves is considered to verify that the combination of equations and concepts in this paper is able to closely reproduce the earlier work conducted by Lundborg. What remains uncertain is whether the crater blasting experiments in Lundborg's work conform to the assumed scaled depth of burial values, since Lundborg did not report the depth of burial or charge size in his experiments. However, it is a relatively simple matter to adjust the K_v v *SDB* correlations according to field data, and in this way obtain independent verification or calibration of the flyrock model.

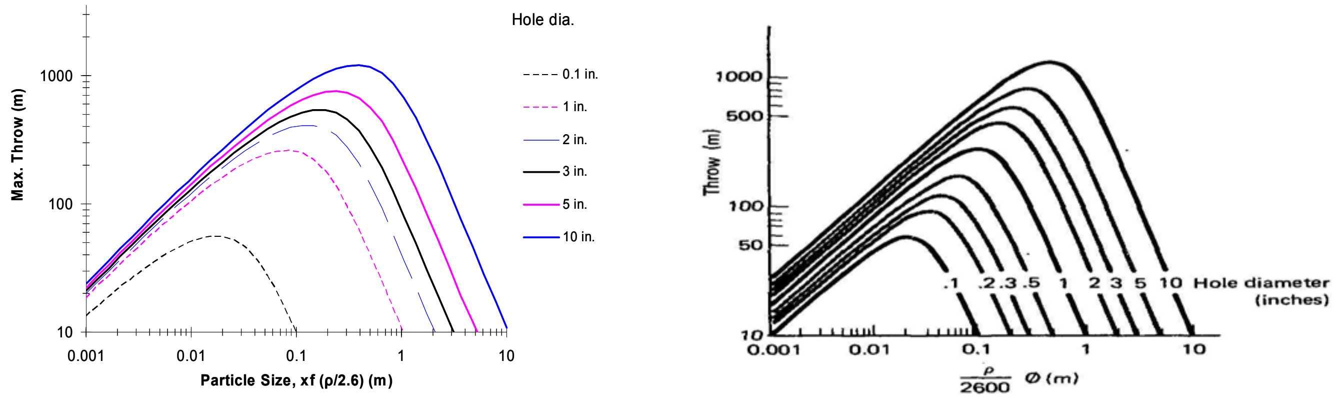

Figure 4. Flyrock "footprint" comparison with current model (left, with SDB_m = 0.594) and work published by Lundborg et al, 1975 (right).

It is noted that solving Chernigovskii's equations requires numerical iteration, which is not convenient for many blast design engineers. As a result, this study aimed to find relatively simple equations to help determine the relationship between flyrock range, particle size, particle shape, and the charge configurations loaded into blastholes.

By coupling the Chernigovskii equations (which calculate particle trajectories as a function of launch velocity, V_0) with the Lundborg/scaled depth of burial equations (which estimate the launch velocity V_0 for variable charge and burial configurations), it becomes possible to estimate the particle trajectories for charges of variable depth of burial (i.e. with different stemming lengths). A series of 1024 simulations was conducted, in which blasthole diameter was varied over the range 76 mm to 380 mm, rock density was varied over the range 1.4 to 4.2 g/cc, particle shape factor was varied over the range 1 to 1.6, and stemming was varied over the range 4 to 43 times blasthole diameter. In these simulations, the Chernigovskii equations were used to find the maximum projection distance and the particle size which produced the maximum projection distance, and the Lundborg/SDB equations used to estimate launch velocity, V_0. The resulting simulations were used to develop scaling equations to describe particle projections. In Figure 5, the maximum projection distances for all 1024 simulations are seen to lie on a single curve of the same form as that reported by Lundborg (equation 1), but the equation is modified to include the variable influences of the launch velocity coefficient K_v, and particle shape factor, F_s. With reference to the equation parameters displayed in Figure 5, Lundborg's maximum range equation (1) can be rewritten:

$$Range_{max} = 62.9 \left(\frac{K_v}{F_s} \right)^{0.667} \phi^{0.667} \tag{7}$$

This means that Lundborg's *Range Coefficient* (equal to 260, equation 1) to estimate maximum projection distance can be rewritten to account for different stemming lengths and different shape factors for the projected fragments:

$$Range\ Coeff = 62.9 \left(\frac{K_v}{F_s} \right)^{0.667} = \frac{11 \times SDB^{-2.167}}{F_s^{0.667}} \tag{8}$$

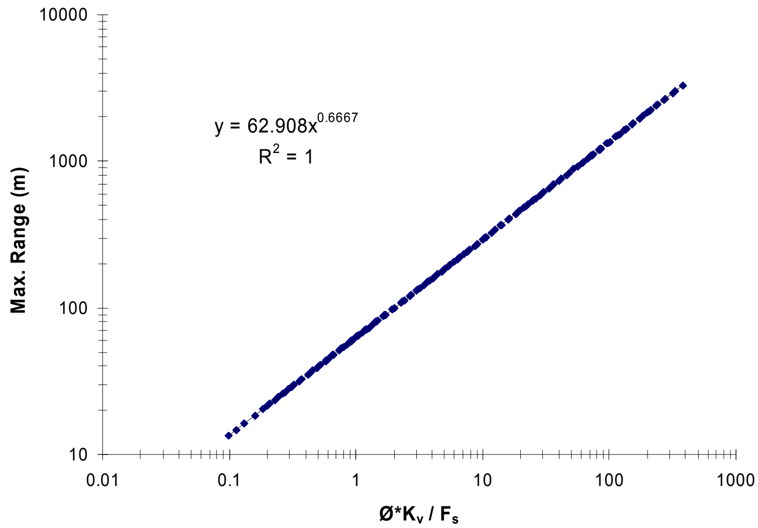

Figure 5. Max. flyrock range as a function of hole dia (ø), shape factor (F_s), and the launch velocity coefficient (K_v).

Coupling this equation with the assumed K_v v *SDB* curve produces the alternative form of Lundborg's equation (1):

$$\therefore\ Range_{max} = 11 \times SDB_m^{-2.167} \left(\frac{\phi}{F_s} \right)^{0.667} \qquad (9)$$

where ø is the hole diameter measured in mm, F_s is the Shape Factor, $Range_{max}$ is measured in metres, and SDB_m is the metric form of the scaled depth of burial equation.

The perfect correlation of the curve implies that for any flyrock projection, from a blasthole of any stemming length, for any charge configuration and for any particle shape factor, the maximum distance of projection can be calculated from the above equation. For a metric scaled depth of burial = 0.594 (crater blasting condition), and a shape factor of 1.2, the above equation produces the same curve (i.e. equation 1) reported by Lundborg *et al* (1975). For a metric scaled depth of burial = 1.386 ("normal" bench blasting condition), and a shape factor of 1.2, the above equation produces maximum projection distances equal to approximately one sixth of those observed in crater blasting, consistent with the observations of Lundborg. For a metric scaled depth of burial = 2.376 (stemming length equal to 40 times the hole diameter, metric units), and a shape factor of 1.2, the above equation predicts projection distances of a few metres, generally consistent with Lundborg's observations. The above equation can easily be implemented in a spreadsheet and incorporated into the blast design process to provide estimates of maximum projection range for any charge configuration and blasthole diameter.

In the same way that Figure 5 presents a useful curve for estimating maximum projection range for any charge configuration and particle shape factor, a similar curve exists which ultimately enables estimation of the size of particle which achieves the maximum projection distance. For each of the 1024 simulations mentioned above, involving a wide range of particle sizes, rock densities, scaled depths of burial, and shape factors, the size of the particle which achieved maximum projection, and its launch velocity were noted to always follow exactly the same trend as presented in Figure 6.

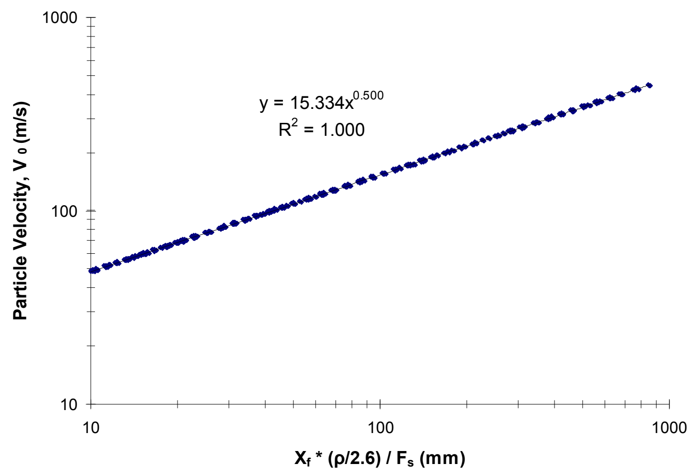

Figure 6. Size of rock fragment which achieves maximum projection distance as a function of rock density (ρ), shape factor, F_s, and the launch velocity, V_0.

Combining the modified impulse equation (6), with the trend of Figure 6 produces:

$$V_0 = 72.8 \times SDB^{-3.251} \times \left(\frac{\phi}{x_f}\right)\left(\frac{2.6}{\rho_r}\right) = 15.334 \times \left[\left(\frac{x_f}{F_s}\right)\left(\frac{\rho_r}{2.6}\right)\right]^{0.5}$$

After rearrangement, the equation to estimate the size of the particle capable of achieving maximum projection distance can be calculated as a function of the scaled depth of burial, and is given by:

$$x_f\left(\frac{\rho_r}{2.6}\right) = 2.82 \times SDB_m^{-2.167}\,\phi^{0.667}F_s^{0.333} \qquad (10)$$

in which the influence of particle density can now be seen. Particle density does not affect the maximum projection range of particles, but it does affect the size of particles which can achieve the maximum range.

Importantly, equations (7), (8) and (9) can only be used to calculate the maximum projection distance of a particle of size given by equation (10). The equations can not be used to estimate the range of particles of any other size. As a further note, the angle of projection which produces the maximum projection range in reality is not 45 degrees, as is the case under conditions of simple kinematic motion. The angle of projection which produces the maximum range is a complex function of particle size, shape factor and launch velocity, as shown in Figure 7, which is asymptotic to 45 degrees for low projection velocities and larger particle sizes. Figure 7 includes all 1024 simulations as previously outlined.

It is noted that the equations of Chernigovskii show that the angle of projection which produces the maximum projection distance is less than 45 degrees as a result of including the effects of air resistance, in contrast with the findings of St George & Gibson (2001). The equations of Chernigovskii, and the conclusion that the projection angle for maximum throw decreases from 45 degrees as a result of air resistance, however, are consistent with other work, such as the web applet:
http://www.phy.davidson.edu/StuHome/jocampbell/projectile/projectile.ProjectileControl.html.

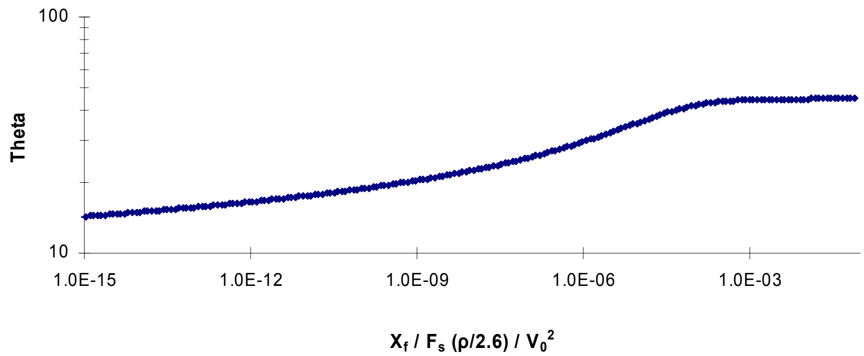

Figure 7. Projection angle which produces maximum projection range, as a function of particle size, shape factor, density and launch velocity.

Applications in Blast Design

The obvious applications for a flyrock model in blasting are:

1. to assist with determining appropriate personnel clearance distances;
2. to determine appropriate changes to charge design when blasting in close proximity to occupied or otherwise sensitive structures;
3. to evaluate risks associated with equipment which remains inside the flyrock projection zone.

This section examines the first two applications, with the third being the topic of a later paper. In applying the guidelines in this paper to establish appropriate clearance distances, the following issues are of paramount importance:

1. actual charge configurations are never the same as the design configurations;
2. the clearance distance is only effective if the actual charge conditions are known and accounted for;
3. the gravest error as regards an overcharged hole is unawareness, or failure to take appropriate action.

Personnel Clearance Distance

Lundborg *et al* (1975) were absolutely correct when they stated "*People must be protected against flyrock, no matter what the cost.*" Given that flyrock projection distances can and have exceeded 1 kilometre (Figure 4), the selection of a clearance distance must be carefully undertaken with full knowledge of the particular blasting application. Typically, quarries and small blasting operations apply a personnel clearance zone of between 100 and 300 metres. Large mines usually adopt a personnel clearance zone of at least 500 metres. These distances, however, seem very arbitrary, especially considering the variability in blasting conditions between different operations and even different blasts within the same operation, whereas the issue of maintaining personnel safety demands a strong engineering basis to ensure safety under all blasting conditions at all times.

A recommended procedure is to use the prediction of the maximum projection range as the basis for determining clearance distance, with an appropriate Factor of Safety applied. Clearly, this estimation must be conducted with full knowledge of the length of stemming and actual charge configurations in every blasthole, and distances adjusted according to the particular charge configuration with the largest estimated projection distance.

Where holes contain multiple charge types (e.g. a high density base charge and a lower density column charge), the SDB calculations should be based on the effective or average explosive density. A greater degree of conservatism will result if the calculations are based on the highest density component, even if it is located at the base of the blasthole. Similarly, if a charge contains air (e.g. an air deck or decoupled cartridge product), then the effective density should be calculated by distributing the known weight of explosive over the full "active" column length (i.e. charge length plus length of air deck). In this way, the effect of charge decoupling on flyrock projection can be included in the calculations. The inclusion of an air deck in the charge column is not in itself a guarantee that flyrock will be controlled or eliminated.

Once the maximum projection distance has been calculated, an appropriate factor of safety should be applied. The need for a factor of safety is highlighted by Chernigovskii (1985) in his statement "*Calculations indicate that the trajectory of a fragment cannot be calculated with higher than 20% accuracy because neither the vector of initial velocity of projection v_0 nor the drag factor b_d is correctly known.*". A minimum value for the factor of safety is therefore considered to be 150%, i.e. the clearance distance should be at least 1.5 times the calculated maximum projection distance (Figure 8). Using this design methodology, appropriate minimum personnel distances are presented for different charge configurations in Table 1 and Figure 9. The US Office of Surface Mining (Dick et al, 1989) prohibit throwing flyrock more than one-half the distance to the nearest dwelling or occupied structure, demanding that a minimum Factor of Safety of 2 be used in the US.

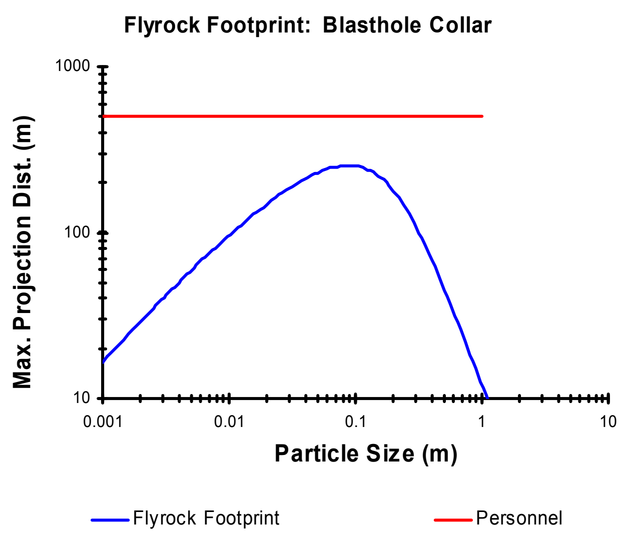

Figure 8. Personnel clearance according to estimated maximum projection distance, with minimum of 150% factor of safety.

With respect to the measurement of stemming length, various authors (Chiappetta, 1983, Sterner, 2003) have suggested that soft soil or overburden in the collar region should not be included in the measurement of stemming length. The length of stemming used to calculate the scaled depth of burial should therefore be the length in rock of reasonable competence.

Table 1. Personnel clearance distances for different blasting conditions (ρ_{exp} = 1.2 g/cc, ρ_r = 2.6 g/cc , factor of safety = 150%, particle shape factor = 1.25).

Ø = 89 mm		Ø = 127 mm		Ø = 165 mm		Ø = 270 mm		Ø = 311 mm	
Stem Length	**Clearance**	**Stem Length**	**Clearance**	**Stem Length**	**Clearance**	**Stem Length**	**Clearance**	**Stem Length**	**Clearance**
1.2	378	2.0	373	2.50	473	4.0	681	5.0	655
1.4	295	2.3	295	3.00	349	4.5	561	5.5	558
1.6	236	2.6	239	3.50	267	5.0	470	6.0	481
1.8	193	2.9	197	4.00	211	5.5	399	6.5	419
2.0	160	3.2	165	4.50	170	6.0	342	7.0	368
2.2	135	3.5	140	5.00	140	6.5	297	7.5	325
2.4	115	4.0	110	5.50	117	7.0	259	8.0	289
2.6	99	4.5	88	6.00	100	8.0	203	9.0	233

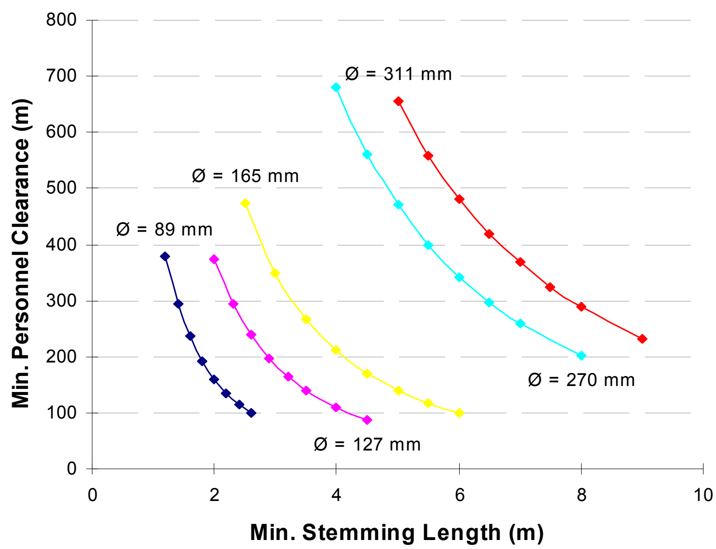

Figure 9. Personnel clearance distances for different blasting conditions (ρ_{exp} = 1.2 g/cc, ρ_r = 2.6 g/cc, factor of safety = 150%, particle shape factor = 1.25).

Based on experience with quarries utilising small diameter blastholes, and mines with large diameter blastholes in a wide range of rock conditions, the minimum clearance distances in Table 1 and Figure 9 do not seem unreasonable. Importantly, they provide a means of either adjusting charging configurations to suit fixed clearance distances, or of adjusting clearance distances to suit charging conditions.

Blasting Close to Sensitive Structures

On occasion it is necessary that blasting operations be conducted close to occupied structures, and further, that such structures can not be evacuated. Alternatively, blasting may be conducted close to some other type of sensitive, fixed structure (pipeline, power lines, water storage tanks, primary crusher etc). In such cases, the only remaining option for the blasting engineer is to adjust the charge configuration so as to ensure that the projection of fragments is strictly contained. In such cases, the control of flyrock assumes greater priority than the achievement of perfect fragmentation. This compromise must be recognised by the blasting management, since the methods to control and contain the blast energy will frequently result in a general coarsening of the resulting fragmentation.

To determine appropriate stemming lengths, Table 1 and Figure 9 can again be used. If the nearby sensitive structure is occupied, then the factor of safety of 1.5 should be retained. If the sensitive structure is sturdy equipment, then the factor of safety can be reduced, though the risks should be carefully evaluated before making such reductions. An expression to calculate the minimum stemming length, St_{min}, for a sensitive receiver at distance *Dist*, incorporating all terms including the Factor of Safety (*FoS*) is found by simple re-arrangement of terms:

$$St_{min} = 0.028 \frac{\left(m\rho_{exp}\right)^{0.33} \; \phi^{1.308}}{\left(\dfrac{Dist}{FoS}\right)^{0.46} \; F_s^{\,0.308}} - 0.0005 \times m \times \phi \qquad (11)$$

where ø is measured in mm, both *Dist* and St_{min} are measured in metres, the effective explosive density ρ_{exp} is measured in g/cc, and for which a reasonable value of the shape factor is 1.2 (a value of 1.0 will give a more conservative estimate of minimum stemming length), and a minimum factor of safety (for personnel) should be 1.5. As outlined previously, *m* is the ratio of charge length to hole diameter but has a maximum value of 8 for holes of diameter less than 100 mm, and 10 for holes of diameter greater than or equal to 100 mm.

The Human Factor

As in most processes, the Human Factor can often be the weak link in the process of controlling flyrock. The main area in which human error can foil an otherwise good outcome is in the quality control of charging. Quality control during charging becomes increasingly important the closer blasts are to sensitive structures. In particular, stemming lengths (excluding any zone of unconsolidated soil or overburden) play a critical role, requiring constant focus on the following issues:

1. explosive columns should never be longer than design to such an extent that estimated maximum flyrock projections can exceed two thirds of the distance to sensitive receivers;
2. explosive column density should not be significantly higher than design – either through incorrect gassing of emulsion products, errors in the size of high density base charges, reductions in size of air decks, or the use of larger diameter cartridge products than was proposed in the design (where an air deck is specified, but the hole is full of water, then calculations of effective explosive density should ignore the air/water deck);

3. stemming columns must be continuous, and bridging of the stemming columns must be avoided – best achieved through the use of uncontaminated, graded aggregate material, and loaded so as to avoid bridging;
4. strict and clearly-defined protocols for exception reporting – errors will happen, and adjustments to procedures can be made providing that the error is reported and tools are available to provide reliable estimates of worst case outcomes.

A simple statistical analysis of normal charging operations (e.g. measurement of stemming column length for a hundred or more holes) will always reveal error and variability in the length of stemming columns. Assuming a Normal Distribution of such errors, stemming lengths should be considered to have a mean value St_{avg} (hopefully close to the design value), as well as a standard deviation, σ_{st}. When calculating the value of *SDB* in the above equations, users should use at least a 95 percentile value of the stemming length *St*, i.e. the stemming length, St_{95}, which is exceeded by 95% of holes in the pattern:

$$SDB_m = \frac{St_{95} + 0.0005\, m\phi}{0.00923\left(m\phi^3 \rho_{exp}\right)^{0.333}} = \frac{St_{avg} - 1.64\,\sigma_{st} + 0.0005\, m\phi}{0.00923\left(m\phi^3 \rho_{exp}\right)^{0.333}} \qquad (12)$$

A normal degree of variability in stemming length would be around 10%, i.e. if the design stemming length was 5 metres, the standard deviation of the errors in length is probably around 0.5 metres, and the value of stemming length used in calculating *SDB* should therefore be around (5 - 1.64 x 0.5) = 4.2 metres, or 84% of the designed stemming length. This approach, combined with a Factor of Safety of 1.5 with the clearance distance, should guarantee the safety of all in the vicinity of the blast.

It must be remembered that if one blasthole in a pattern is badly loaded, the safety of all in the vicinity is compromised. The failure in a blast which produces flyrock is not so much the error in charging which produced the flyrock, but the lack of awareness and failure to respond appropriately to the error by those in charge of loading and firing the shot.

Examples of Application

Table 2 presents examples of both maximum projection distance and safe personnel clearance distance, for a range of different blasthole diameters and charge configurations, generally covering international quarrying practices and mining practices.

The distances shown in Table 2 seem to be in good agreement with general quarry and mining practice over the range of hole diameters 100 mm (4 inch) to 350 mm (13¾ inch), for explosive densities commonly used. Note also that as the maximum projection distance increases, so too does the size of rock capable of being projected that distance. The estimates are derived for a fixed bench height of 15 metres (50 ft), and a fragment shape factor of 1.25, and the minimum personnel clearance distance is based on a factor of safety of 1.5 times the maximum estimated projection distance.

Table 2. Maximum projection range and clearance distance for some quarry and mining charge configurations.

Hole dia. mm (in)	Chg. Density (g/cc)	Stem Length m (ft)	Max. Range m (ft)	Fragment Size mm (in)	Min. Clearance m (ft)
102 (4.0)	1.2	2.0 (6.6)	130 (430)	50 (2.0)	200 (650)
102 (4.0)	1.2	2.5 (8.2)	90 (300)	30 (1.2)	135 (450)
102 (4.0)	0.8	2.5 (8.2)	70 (230)	20 (0.75)	105 (350)
140 (5.5)	1.2	2.5 (8.2)	220 (720)	70 (2.75)	330 (1100)
140 (5.5)	1.2	3.0 (10)	160 (520)	50 (2.0)	240 (800)
140 (5.5)	0.8	3.0 (10)	120 (400)	40 (1.8)	180 (600)
270 (10⅝)	1.2	4.5 (15)	380 (1250)	130 (5.1)	570 (1900)
270 (10⅝)	1.2	5.5 (18)	270 (900)	90 (3.5)	400 (1300)
270 (10⅝)	0.8	5.5 (18)	210 (700)	70 (2.75)	320 (1050)
350 (13¾)	1.2	6.5 (21)	370 (1200)	130 (5.1)	560 (1800)
350 (13¾)	1.2	7.5 (25)	290 (950)	100 (4.0)	440 (1400)
350 (13¾)	0.8	7.5 (25)	230 (750)	80 (3.1)	350 (1100)

Limitations of the Model

While the model described in this paper presents a significant step forward in terms of engineering design, and the ability to better understand some of the many factors influencing flyrock, some factors are still unaccounted for. Such factors include:

1. the influence of stemming material (drill cuttings v crushed aggregate);
2. the effect of delay timing and confinement issues within the blast;
3. primer location in the explosive column;
4. the impact of water in the blasthole and saturated ground conditions.

It is noted that the model predicts flyrock ranges which sometimes appear greater than expected and greater than generally observed. Short stemming lengths (e.g. less than 18 times the blasthole diameter) are quite commonly used even with quite high density and high energy explosives, often with little observed collar flyrock. It should first be stated that not every incidence of stemming ejection produces a rock fragment at a trajectory which will result in large projection distances. Further, video records of such outcomes generally include a free face, from which the burden material moves quite quickly, relieving the pressure on the stemming column as well as its duration of application, thereby lowering the probability of ejections. The model may therefore be most useful to indicate flyrock range under conditions which result in over-confinement of the charges (e.g. misfires, out-of-sequence initiation, over-burdening of charges, etc). In order to design a blast which will be safe even under conditions of high confinement (i.e. fail safe), the model appears to be a very useful tool.

While the model lacks recent data to confirm its validity, it passes the test of reproducing all of Lundborg's field observations which represent one of the few well-documented field flyrock studies. Obtaining data to confirm the model does not seem difficult with high speed digital cameras readily available, together with software to quickly determine particle velocities. Such studies could focus either on the collar region of holes, or on the free face. The model is considered easy to adjust, or calibrate, according to such field data, with the primary area of adjustment likely to be the relationship between the velocity coefficient, K_v, and the scaled depth of burial, *SDB*.

Conclusions

Flyrock generation from around the collars of blastholes depends on a range of conditions including length of stemming, blasthole diameter, charge length, and explosive density. Once generated, the maximum projection distance of flyrock fragments depends on fragment size, material density, and fragment shape factor. While kinematic models are unable to account for most of these factors, the model presented in this paper permits estimation of flyrock projection distance as a function of all of these factors.

The primary underlying assumption of the model is the relationship between flyrock ejection velocities and the scaled depth of burial – an assumption which appears quite readily adjustable through quite simple field studies with high speed cameras.

The model as it is presented appears to provide quite realistic clearance distances for known charge configurations, or the ability to adjust charging configurations to suit situations where sensitive receivers such as houses at fixed distances must be protected against flyrock damage.

Alternatively, the model can be used to determine appropriate stemming lengths in situations where blasting must be conducted close to occupied structures or other sensitive structures which could include plant such as excavators or drills. When used to estimate stemming lengths, users must account for realistic variability in the length of stemming columns (e.g. due to variable product gassing), and the measured length of stemming should ignore soft or unconsolidated overburden material.

Several important issues remain unaccounted for in the model, including primer location within the explosive column, the effect of stemming material, the effect of water in the blastholes, and the effect of delay timing.

The model lends itself to quantification of the risk of damage from flyrock, as a function blast design, quality control over design implementation, distance from sensitive receivers, and the size (length, width and height) of sensitive receivers.

References

Chernigovskii, A.A., 1985. “Application of directional blasting in mining and civil engineering”, Chapter 4 Movement of Flyrock Subject to Air Drag, pp 91-100.

Chiappetta, R., Bauer, A., Dailey, P. and Burchell, S., 1983. “The Use of High-Speed Motion Picture Photography in Blast Evaluation and Design”, Proceedings of the Ninth Annual Conference on Explosives and Blasting Technique. Dallas, TX. International Society of Explosives Engineers, pp 258-309.

Dick, R.A., Fletcher, L.R, & D'Andrea, D.V., 1989. “Explosives and Blasting Procedures Manual, Chapter 5, Environmental Effects of Blasting”, USBM IC 8925e, 14p.

Lundborg, N., 1974. "The hazard of flyrock in rock blasting", Swedish Rock Blasting Committee, Stockholm, Sweden.

Lundborg, N., Persson, P-A., Ladegaard-Pedersen, A. and Holmberg, R., 1975. "Keeping the Lid on Flyrock in Open-pit Blasting", Engineering and Mining Journal, 176:95-100.

Richards, A.B., & Moore, A.J., 2006. "Environmental Blast Simulation", International Symposium on Rock Fragmentation by Blasting, Fragblast 8, Santiago, Chile, May, pp271-278.

Roth, J., 1981. "A model for the determination of flyrock range as a function of shot conditions", United States Department of the Interior, Contract No. JO387242, OFR 77-81.

Sterner, V. A., 2003. "Trench Blasting Patterns & Pitfalls", Blasters' Training Seminar, February 1-2, Nashville, TN: International Society of Explosives Engineers.

St George, J.D., and Gibson, M.F.L., 2001. "Estimation of Flyrock Travel Distances: A Probabilistic Approach", AusIMM EXPLO 2001 Conference, Hunter Valley, pp409-415.

Workman, J.L, and Calder, P.N., 1994. "Flyrock prediction and control in surface mine blasting", Proceedings of 20th Annual Conference on Explosives and Blasting Technique, International Society of Explosives Engineers, Austin, Texas, USA.